Received: 10 April 2022 | Revised: 31 October 2022 | Accepted: 2 November 2022

DOI: 10.1002/hyp.14760

RESEARCH ARTICLE

WILEY

Spatial variation of grassland canopy affects soil wetting patterns and preferential flow

Gökben Demir[1] | Beate Michalzik[2,3] | Janett Filipzik[1] | Johanna Clara Metzger[1] | Anke Hildebrandt[1,3,4]

[1]Group Terrestrial Ecohydrology, Institute of Geoscience, Friedrich Schiller University Jena, Jena, Germany

[2]Chair of Soil Science, Institute of Geography, Friedrich Schiller University Jena, Jena, Germany

[3]German Center for Integrative Biodiversity Research (iDiv) Halle-Jena-Leipzig, Leipzig, Germany

[4]Department of Computational Hydrosystems, Helmholtz Centre for Environmental Research – UFZ, Leipzig, Germany

Correspondence
Gökben Demir, Group Terrestrial Ecohydrology, Institute of Geoscience, Friedrich Schiller University Jena, Jena, 07749, Germany.
Email: goekben.demir@uni-jena.de

Funding information
Deutsche Forschungsgemeinschaft, Grant/Award Number: 218627073

Abstract

Canopies shape net precipitation patterns, which are spatially heterogeneous and control soil moisture response to rainfall. The vast majority of studies on canopy water fluxes were conducted in forests. In contrast, grassland canopies are often assumed to be spatially homogeneous, therefore likely not inducing patches of heterogeneity at and below the soil surface. However, some studies on short-structured vegetation, such as grasslands, proposed the importance of canopy-induced heterogeneity for net precipitation. Still, systematic investigations on the effects on soil wetting patterns are missing. Therefore, in this study, we investigated soil moisture response to rainfall in a managed temperate grassland by exploring the individual impacts of spatially varying throughfall, vegetation height, and antecedent soil moisture status on the soil wetting patterns. We applied linear mixed effects models to disentangle the role of grassland canopy versus abiotic drivers. The spatial average soil water response showed diminishing water amounts stored in the upper parts of the soil as the growing season progressed and the soils dried, indicating bypass flow. Spatial variation of grass height was a significant driver of soil wetting patterns along with precipitation and antecedent soil moisture status. Soil wetting was suppressed in locations with tall canopies, although surprisingly, this was not directly related to throughfall patterns. Instead, our results suggest that seasonally drier conditions and the spatial difference in grass development amplify fast flow processes. Ultimately, our results confirm that spatial variation of the canopy affects soil moisture wetting patterns not only in forests but indicate a strong influence of preferential flow on soil water patterns in managed grassland as well.

KEYWORDS
grassland, interception tubes, preferential flow, soil moisture, throughfall patterns

1 | INTRODUCTION

Vegetation regulates how precipitation arrives at the soil surface as it intercepts and redistributes precipitation. While the intercepted portion evaporates back into the atmosphere, net precipitation enters the soil in the forms of throughfall and stemflow. Net precipitation components are shaped by vegetation features such as canopy storage capacity, leaf area index, crown size, leaf shape and orientation,

branch angle, canopy gaps, stem surface structure (Levia & Frost, 2006; Levia & Germer, 2015; Pypker et al., 2011), and canopy height particularly in short vegetation (Crouse et al., 1966; Demir et al., 2022). While throughfall may or may not touch the canopy and drips to the ground, stemflow reaches the ground as concentrated flow along the stems (Crockford & Richardson, 2000). Throughfall is typically the higher fraction of gross precipitation and, depending on climate and vegetation type, amounts to roughly 75% of rainfall (Sadeghi et al., 2020).

Precipitation is the primary source of soil wetting, particularly for topsoil layers (Lozano-Parra et al., 2015; Salve et al., 2011; Zhang et al., 2020; Zhu et al., 2014). However, soil wetting and net precipitation do not always exhibit a similarly strong relationship as observed for other variables, e.g., the relationship between soil properties and soil water content (Jarecke et al., 2021). For example, Molina et al. (2019) observed a strong relationship between soil moisture response and throughfall in two oak and pine-dominated forest sites in a Mediterranean climate. However, they also found decoupling between soil wetting dynamics and throughfall amount during stronger rain events. They argued that drier antecedent soil moisture conditions induced alternative flow paths, suppressing soil water recharge. In addition, Metzger et al. (2017) found in a mixed forest that spatial patterns of net precipitation were only reflected in soil water patterns of a small subset (one-third) of the observed events. Indeed, next to soil properties, soil moisture patterns were controlled by antecedent soil wetness and preferential flow (Lozano-Parra et al., 2015; Tian et al., 2019; Vereecken et al., 2007, 2014; Zhang et al., 2020). Especially dry soils can cause water repellence or lead to shrinking, thus enhancing preferential flow (Beven & Germann, 2013; Jarvis, 2007; Nimmo, 2021). Compared to the spatial variation of net precipitation, research on the role of canopy processes on soil hydrology is much rarer and has mostly been performed in forests and shrublands (e.g., Bouten et al., 1992; Jian et al., 2018; Li et al., 2009; Metzger et al., 2017; Molina et al., 2019), while small structured vegetation communities are underrepresented (Dunkerley, 2000; Llorens & Domingo, 2007; Sadeghi et al., 2020). In forest ecosystems, it was investigated partly by using model-based approaches and field observations on how canopy-modified net precipitation patterns influence soil water content or soil water fluxes (Coenders-Gerrits et al., 2013; Guswa, 2012; Klos et al., 2014; Metzger et al., 2017). For instance, at the forest site adjacent to this grassland study site with intensive observations, Metzger et al. (2017) showed that soil moisture patterns responded to throughfall patterns, yet the correlation between soil wetting and throughfall patterns was weak and momentary.

It has been shown that short vegetation communities, such as grassland and cropland, also influence soil water dynamics at both plot scales (Baroni, 2013; Teuling et al., 2007) and catchment scales (Gómez-Plaza et al., 2000; Teuling & Troch, 2005). In a maize field, for instance, Baroni (2013) observed that soil moisture variability in the topsoil was governed by features of the maize vegetation, namely leaf area index and vegetation height, when soil conditions were dry or moderate due to the shading effects of the vegetation. Further, Teuling and Troch (2005) demonstrated through model simulations for three different sites featuring small structured vegetation (cropland, grassland, perennial pasture) that vegetation activity becomes the major driver affecting soil water spatial variability, particularly at dry and medium soil wetness. These studies indicate that next to forests and shrubs, canopy-related structural heterogeneity can modify soil water dynamics also in short vegetation communities. However, these investigations focussed on the evapotranspiration between precipitation events at large scales, not small-scale net precipitation patterns. To the best of our knowledge, investigations on the impact of net precipitation patterns on soil hydrology in grasslands are absent. Therefore, we here explore canopy and soil wetting patterns together with the impact of soil moisture conditions on the plot scale in concert with different biotic and abiotic factors. Demir et al. (2022) recently showed that grass canopies systematically affect throughfall patterns and generate heterogeneity in water input at the ground level. Here, we take it one step further to understand how net precipitation components influence soil moistening patterns in grasslands, and we pose the following research questions:

1. Does grassland canopy-induced variation in water input influence soil wetting patterns?
2. How does the antecedent soil moisture status affect the soil moisture response to rainfall?

We address these questions by using a statistical model based on field measurements in grassland in a temperate climate.

2 | MATERIALS AND METHODS

2.1 | Research site and field measurements

Our research site is a managed temperate grassland (0.045 ha) that is mown 2–3 times per year, and it is part of the Hainich critical zone exploratory (CZE), located in central Germany (Thuringia) (Küsel et al., 2016). The grassland plant community at the site is similar to the neighbouring plot where the plant community was characterized by different functional groups such as graminoides (e.g., *Dactylis glomerata*), legumes (e.g., *Trifolium repens*), and herbs (e.g., *Taraxacum spec.*) (Potthast et al., 2017). The annual average precipitation in the region is around 600 mm, and the annual mean temperature varies around 9.0°C (Küsel et al., 2016). The main soil type in the Hainich CZE and a nearby pasture is Calcaric Cambisol (Siltic) developed from carbonate rocks (German Triassic Muschelkalk formations) and aeolian deposits (Kohlhepp et al., 2017; Potthast et al., 2017). The soil depth to the weathered bedrock in the research site varies between 17 and 51 cm, yet the median soil depth is 30 cm.

The grassland site was equipped with a soil moisture measurement network (SoilNet; Bogena et al., 2010) composed of SMT100 frequency domain sensors (Truebner GmbH, Neustadt, Germany). The sensors were installed based on a nested triangular schema at 30 locations for two depths (7.5 and 27.5 cm). At the research site, the soil moisture setup installation was completed in 2016, and it provides

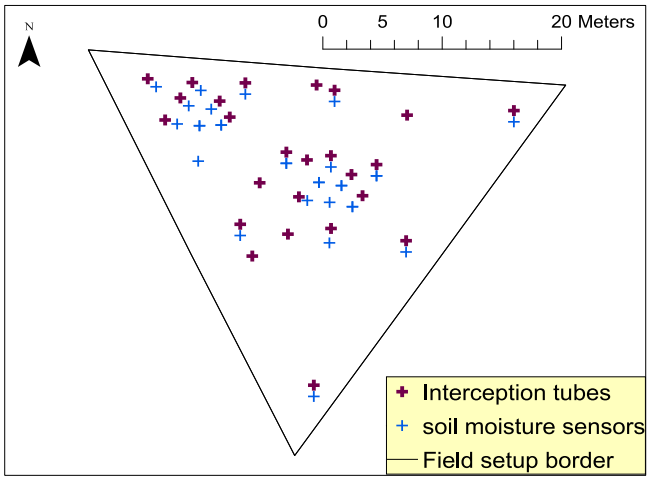

FIGURE 1 Field setup of the interception tubes and soil moisture sensors

high temporal resolution data (every 6 min). Unfortunately, sensors started failing within two years of the installation.

We installed 25 interception tubes in early spring 2019 to measure net precipitation (Figure 1). The interception tubes are an in-situ device to measure net precipitation in herbaceous vegetation in a temperate climate. The design is described in Demir et al. (2022). Shortly, it consists of four thin, partly opened plexiglass pipes (20 mm in diameter and 360 mm in length, the opening is 12 mm wide and 262 mm) which are connected to a below-ground plastic sampling bottle. The method does not strictly separate stemflow and throughfall by its construction. Depending on canopy development and density, the partly opened pipes collect net precipitation, and collected water flows by gravity into the sampling bottle. The tubes have been shown to represent net precipitation patterns in the grass canopy (Demir et al., 2022). Based on the same nested design, 22 interception tubes were paired with nearby soil moisture sensors and installed down-slope to ensure that net precipitation measurements did not interfere with the soil moisture sensors. The distance between the tubes and the sensor was less than 1.5 m at 18 sampling locations. Some soil sensors could not be paired with interception tubes due to the clustering of some sensors. In order to increase net precipitation sampling points, we installed three additional interception tubes away from the soil moisture sensors.

Furthermore, we installed five gross precipitation collectors mounted ca. 1.5 m height above the ground. The collectors were composed of a plastic circular funnel (12 cm in diameter) and sampling bottle, which is connected at the neck (Metzger et al., 2017; Zimmermann et al., 2010), and evaporation loss from the orifice surface was prevented by placed tennis ball into the orifice. We conducted weekly sampling of interception tubes, gross precipitation collectors, and grass height from March to August 2019. The vegetation canopy was tall enough (h_{grass} > 0.15 m) to cover the tubes for 14 weeks (covered period). In the first weeks of the sampling period and the weeks following the summer cut, the vegetation was too short and sparse to induce interception or canopy redistribution (uncovered period).

2.2 | Data analysis

2.2.1 | Soil water content data quality control

The high-resolution soil moisture data were characterized by multiple failures such as long breaks, jumps to extremely low and high values, and lack of temporal variation despite rain events. Hence, we applied systematic quality control. Each soil moisture sensor time series was visually checked for plausibility. We removed both extremely low (water content <5 vol-%) values and long plateaus of repeated values. Additionally, we excluded the data in case of long interval data breaks, which prevented us from estimating soil moisture response to rainfall events. Nine to 24 (out of 30) topsoil sensors and eight to 23 subsoil sensors met the quality criteria. All quality-controlled data were used to obtain daily and spatially average volumetric soil water content (SWC [vol-%]) throughout the sampling period to examine soil wetness status at the research site. In addition, we used the quality-controlled soil water content data from both top and subsoil sensors to estimate the weekly increase of the spatial average in the soil water storage to calculate the water balance for the monitored soil profile. For the investigation of the interaction between grass canopy and soil moisture response, we used the paired topsoil quality-checked data (10 locations).

2.2.2 | Defining rainfall event and corresponding soil water content increase

We acquired weekly average wind speed and precipitation time series (resolution 10 min) from the nearby Reckenbühl weather station, which is located about 1.4 km distance to the Northeast of the grassland site. Based on the precipitation time series, we separated individual rainfall events by applying a threshold time interval of 8 h between the end of the last and beginning of the next rain event. The threshold was chosen to reflect the time lag between the end of the gross precipitation event and the canopy drip.

Although not specifically indicated, the following equations were applied for individual sensors, for example, for top and bottom sensors separately. We calculated the increase in soil water content, $\Delta\theta_{i,n,w}$, for all defined rain events (n) in the week (w) at each soil moisture sensor location (i) in the topsoil and subsoil. An increase in soil water content was determined as the difference between maximum soil water content during or immediately after the rainfall event ($\theta_{\max\, i,n}$) and the pre-event condition ($\theta_{\mathrm{pre-ev}\, i,n}$). For the latter, we used the minimum soil water content within 2 h before the beginning of rainfall.

$$\Delta\theta_{i,n,w} = \theta_{\max\, i,n} - \theta_{\mathrm{pre-ev}\, i,n}. \quad (1)$$

If multiple events occurred within the weekly net precipitation-sampling interval, we calculated the sum of the individual increases in soil water content corresponding to each event.

$$\Delta\theta_{i,w} = \sum_{n=1}^{n} \Delta\theta_{i,n,w}. \quad (2)$$

In this way, we obtained a weekly cumulative increase in the soil water storage ($\Delta\theta_{i,w}$) due to rain events (n) for each location (i) for all observed weeks (w).

Similarly, we calculated the weekly pre-event soil water content at each location as the average of all pre-event conditions over all events within the sampling week. This information was used to characterize the weekly soil moisture conditions in the following analyses.

$$\overline{\theta_{\text{pre-ev},i,w}} = \frac{\sum_{n=1}^{n} \theta_{\text{pre-ev},i,n,w}}{n}. \quad (3)$$

2.2.3 | Descriptive statistics

Next to the weekly spatial mean of pre-event soil water content, increase in the soil water content, grass height, and the weekly average of wind speed, we used quantile-based metrics to assess spatial variation of the soil moisture status and increase in the volumetric soil moisture data. The coefficient of quartile variation (CQV) was calculated as stated below:

$$\text{CQV} = \left(\frac{Q_3 - Q_1}{Q_3 + Q_1}\right). \quad (4)$$

We also calculated the spatial deviation of soil water content ($\delta\theta_{\text{pre-ev}\,i,w}$) from the spatial mean of pre-event soil water content ($\overline{\theta_{\text{pre-ev},w}}$) per location per week in order to characterize the spatial pattern (Vachaud et al., 1985).

$$\delta\theta_{\text{pre-ev}\,i,w} = \frac{\theta_{\text{pre-ev},i,w} - \overline{\theta_{\text{pre-ev},w}}}{\overline{\overline{\theta_{\text{pre-ev},w}}}}. \quad (5)$$

We similarly determined the spatial deviation of grass height from the mean ($\delta h_{\text{grass},w,i}$) and spatial deviation of net precipitation ($\delta P_{\text{net},w,i}$) per location per week.

2.3 | Water balance

We used a simple soil water balance to estimate how much water was stored in the soil layers over a rain event by exploring the increase in soil water content. For this, we attributed depth 0–17.5 cm to the top sensor and 17.5–37.5 cm to the deeper one. We used the event-based increase in volumetric soil water content calculated in Equation (1) for both top and subsoil and calculated a weighted sum based on the represented soil layer thickness to estimate the event-based increase in stored water volume (ΔS_w) (Equation 7).

$$\Delta S_{i,w} = z_t \sum_{n=1}^{n} \Delta\theta^t_{i,n,w} + z_b \sum_{n=1}^{n} \Delta\theta^b_{i,n,w}. \quad (6)$$

Here z_t is the thickness of the soil column monitored by a top sensor (17.5 cm) and z_b is the thickness of soil represented by a bottom sensor (20 cm), while $\Delta\theta^t_{i,n,w}$ and $\Delta\theta^b_{i,n,w}$ indicate the storage increase in the top and bottom soil moisture sensor at location i at event n in week w.

$$\Delta S_w = \frac{\sum_{i=1}^{i} \Delta S_{i,w}}{i}. \quad (7)$$

As we calculated immediate response to rainfall, we assumed that evapotranspiration was negligible. Therefore, we assumed that water entering the soil is stored in the monitored soil layers or transmitted to a deeper layer.

2.4 | Linear mixed effects model

We applied linear mixed effects models to investigate which variables relate to the increase in soil water content in the topsoil and included potential controlling factors (Table 1). Since the interception tubes have been shown to underestimate the amount of precipitation

TABLE 1 All fixed and random effects included in the linear mixed effects models for estimating the increase in volumetric soil water content ($\Delta\theta_{i,w}$) in the topsoil

Model variables
Single fixed effects
$\overline{P_{g,w}}$ (spatial mean of gross precipitation)
δP_{net} (spatial deviation of net precipitation from the mean)
Z_{tube} (elevation of net precipitation measurement locations)
$\overline{h_{\text{grass},w}}$ (spatial mean of grass height)
δh_{grass} (spatial deviation of grass height from the mean)
$\overline{\theta_{\text{pre-ev},w}}$ (spatial mean of pre-event soil water content)
$\delta\theta_{\text{pre-ev}}$ (spatial deviation of pre-event soil water content from the mean)
$\overline{u}$ (weekly average wind speed)
Interaction fixed effects
$\overline{P_{g,w}} \times Z_{\text{tube}}$
$\overline{h_{\text{grass},w}} \times \delta\theta_{\text{pre-ev,top-soil}}$
$\overline{h_{\text{grass},w}} \times \overline{u}$
$\delta h_{\text{grass}} \times \overline{u}$
$\delta h_{\text{grass}} \times \overline{\theta_{\text{pre-ev},w}}$
$\delta h_{\text{grass}} \times \delta\theta_{\text{pre-ev}}$
Random effects
Sampling date
Soil moisture sensor location

entering the soil (Demir et al., 2022), we used gross precipitation (P_g) to characterize the size of the weekly cumulated events. Yet, we included the spatial deviation of tubes' measurements (δP_{net}) to represent the effect of vegetation-altered precipitation patterns on soil moisture response, as the interception tubes' measurements were capable of catching throughfall patterns (Demir et al., 2022). We accounted for canopy development and heterogeneity directly by including spatial average and spatial pattern in grass height ($\overline{h_{grass,w}}$, $\delta h_{grass,w,i}$). In addition, we included antecedent soil moisture status with spatial average ($\overline{\theta_{pre-ev,w}}$) and the spatial deviation of pre-event soil water content ($\delta\theta_{pre-ev,w,i}$) each calculated per week. Furthermore, we included other abiotic factors, potentially affecting how water enters the soil or soil water dynamics. For this, we considered topography by adding the elevation of net precipitation measurement locations (Z_{tube}) and included weekly average wind speed ($\overline{u}$). Due to the nature of repetitive sampling over fixed measurement locations, we selected measurement dates and soil moisture sensor locations as random effects.

We used *Z*-transformed variables to apply the linear mixed effects model by using the 'scale' function, which is provided in the R base package (R Core Team, 2021). We did all linear mixed effects model analyses with the 'lme4' package (Bates et al., 2015) and we calculated both conditional and marginal R^2 of the model with the 'MuMIn' package (Bartoń, 2020). While conditional R^2 includes the variance of the entire model, marginal R^2 subsumes only fixed effects (Bartoń, 2020).

The best model fit was found using a systematic model selection based on the Akaike's Information Criterion (AIC). We initially included all potential variables together with their interactions (Table 1, "beyond optimal model") to evaluate them based on their level of significance. Only fixed effects were evaluated, and we used the maximum likelihood (ML) to compare the models (Zuur et al., 2009). Model selection was done stepwise, starting with the beyond optimal model. In each evaluation step, we detected the least significant effect (carrying the lowest *p* value) and built the next candidate model without it. We decided whether the removal had a significant effect on the AIC, by on comparing the AIC of the model before and after removing. Only if the AIC was unaffected or increased, the effect was ultimately removed or otherwise retained. The procedure was repeated with the next least significant effect, until all fixed effects were evaluated and the model with the lowest AIC was obtained. Afterward, we refitted the best model with restricted maximum likelihood (REML) (Zuur et al., 2009).

3 | RESULTS

3.1 | Seasonal grass height development and precipitation

We conducted weekly precipitation sampling along with continuous measurements of volumetric soil water content in the growing season of 2019 (April–August). On dates between April 30th and June 26th, July 24th and August 21st, the average grass height was taller than 0.15 m and allowed for sampling of net precipitation with the interception tubes for 14 weekly samplings (Demir et al., 2022). The canopy height exceeded 0.9 m (spatial average) by the end of June. Due to the summer cut (June 26th), the weekly average grass height remained below 0.3 m for the rest of the observation period (July–August, Table 2).

In our sampling period, the larger rainfall events mostly occurred from May to July. However, in June and July, time intervals between rain events were longer compared to early spring. Later in the sampling period, larger events were less frequent (Figure 2a).

TABLE 2 Spatial mean of grass height, cumulative weekly increased soil moisture and quartile of coefficient of variation (CQV) for topsoil

Sampling date	$\overline{h_{grass,w}}$ (cm)	$\overline{\theta_{pre-ev,w}}$ (vol-%)	CQV $\theta_{pre-ev,w}$	$\overline{\Delta\theta_w}$ (vol-%)	CQV $\overline{\Delta\theta_w}$
30 April	20	14.38	0.24	7.37	0.76
07 May	n.a.	15.91	0.27	5.37	0.57
15 May	35	22.6	0.21	16.11	0.28
22 May	46	31.32	0.05	13.95	0.38
29 May	65	23.76	0.14	0.98	0.24
04 June	83	11.27	0.19	0.18	0.52
13 June	92	16.55	0.14	21.57	0.32
18 June	n.a.	32.10	0.08	1.7	0.19
26 June	93	20.55	0.08	0.52	0.19
24 July	n.a.	12.31	0.21	1.5	0.42
30 July	21	9.48	0.37	0.99	0.46
08 August	22	9.93	0.37	2.44	0.39
14 August	26	11.63	0.25	1.98	0.26
21 August	n.a.	11.44	0.25	0.45	0.34

Note: The time interval is based on net precipitation and grass height sampling dates.

3.2 | Soil moisture status and water balance

Throughout the growing season, the soil water content in the topsoil was lower than in the subsoil regardless of canopy cover status (Figure 2a). Early in the growing season, when interception loss was low due to the reduced canopy ($\overline{h_{grass}} < 0.15$ m) the topsoil was wetter than later in the season. While the topsoil exhibited a strong drying response on non-rainy days and small events, the subsoil water status only varied marginally. In the presence of a more developed canopy, however, both soil layers showed a more dynamic wetting-drying response to larger rain events and non-rainy days until the summer grass cut (June 26th). In late June, the soil water content considerably decreased, and soil-wetting signals became weaker in both soil layers. These drier soil moisture conditions persisted throughout the end of the observation period, and the difference in soil moisture status between the two soil layers increased despite several rain events.

Based on the simple water balance, we calculated how much rainfall was stored in the monitored soil layers. Figure 2b shows the increase in soil water storage together with weekly net precipitation and gross precipitation measurements. Note that in periods with tall canopy ($\overline{h_{grass}} > 0.6$ m), the below canopy precipitation was clearly underestimated by the interception tubes, as the net precipitation was smaller than the

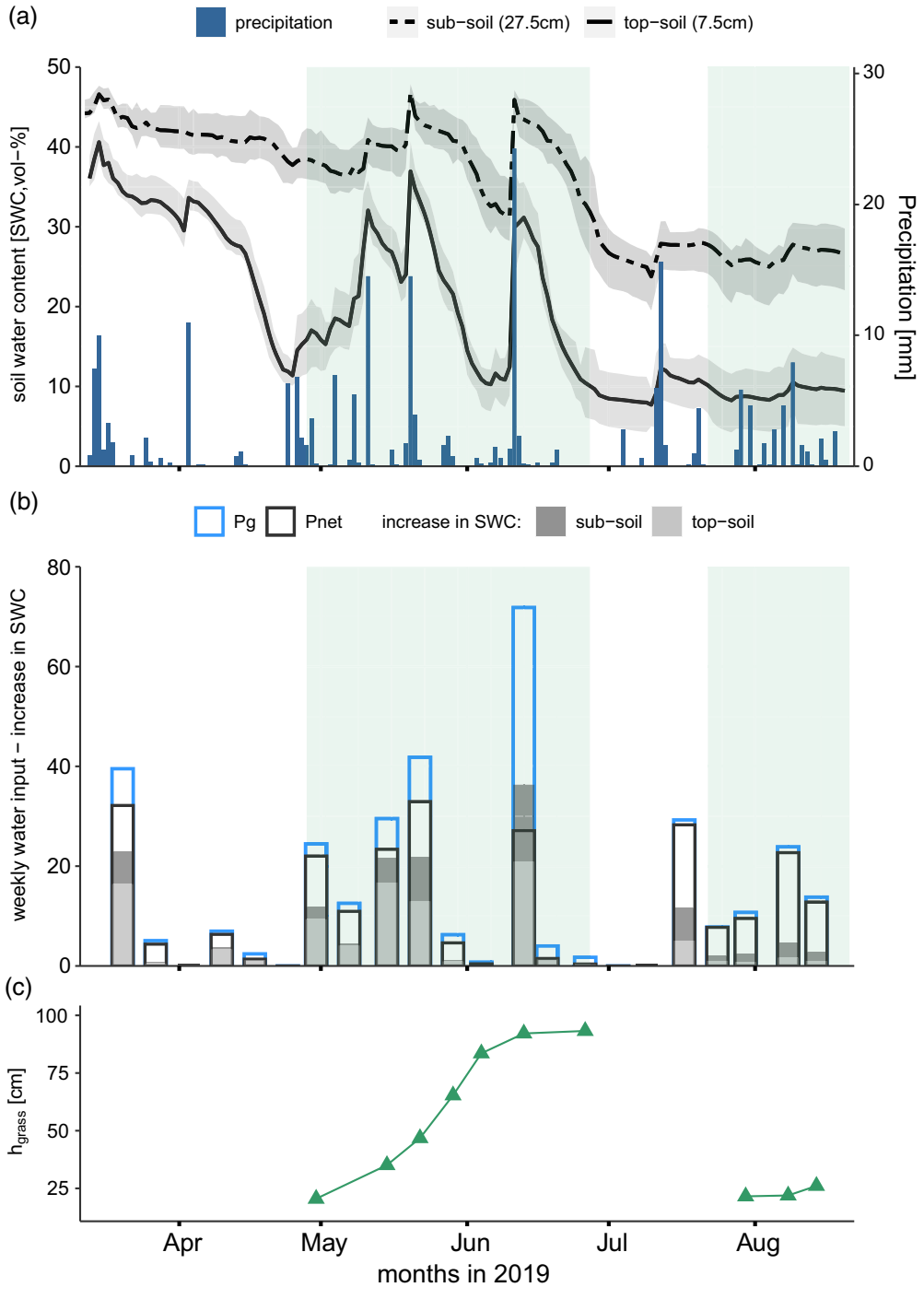

FIGURE 2 (a) Daily volumetric soil water content of top and subsoil and precipitation values from March 13th to August 21st. The solid and dashed lines are; the spatial mean of soil water content estimated based on top (7.5 cm) and bottom (27.5 cm) sensors, and grey shaded areas show the first and third quartiles. Precipitation was measured at the nearby Reckenbühl station (1.4 km to the northeast). (b) Mean of weekly cumulative net precipitation measured with the interception tubes, the difference between funnel measured gross precipitation and the net precipitation, and the increase in soil water content in the top and subsoil. The light and dark grey shaded columns show the increase in the stored water in topsoil (0–17.5 cm) and subsoil (17.5–37.5 cm), respectively. (c) Weekly spatial average of grass height. Only values of h_{grass} > 15 cm are shown; the interruption in the grass height time series is due to the annual mowing.

increase in soil water content. Therefore, we considered the gross precipitation measurements rather than the tubes' measurements as a reference for event size. The increase in soil water storage was always lower than gross precipitation and independent of foliage cover status. While early in the sampling period, until July, still approximately two-thirds of gross precipitation was stored in the monitored soil column (0–37.5 cm), later in the summer, soil layers stored much less than one-third of gross precipitation. This indicates the occurrence of bypass flow later in the season. In addition, the amount of stored water in soil layers after rainfall varied throughout the sampling period. In the presence of a developed canopy, the topsoil retained more rain than the deeper layer, especially in late spring and early summer (Figure 2). However, this switched to the subsoil storing more rain later in the growing season, even after mowing, and despite the drier topsoil conditions. This also indicates preferential flow in the topsoil. Under the presence of a developed canopy, the weekly mean of pre-event volumetric soil water content in the topsoil ranged from more than 30% to around 10% (Table 2). The coefficient of quartile variation (CQV) of pre-event soil water content varied between 0.08 and 0.37, whereas the CQV for the increase in soil water content was much higher and ranged from 0.19 to 0.76. CQV of pre-event soil moisture increased in drier soil conditions. Yet, the CQV of increase in soil water storage was mostly unrelated to the pre-event soil moisture status and the increase in soil water content itself. In other words, the spatial variation of soil wetting could be explained by neither the antecedent soil moisture status nor the amount of water entering the soil.

3.3 | Drivers of spatial patterns of soil water content increase

We used a linear mixed effects model to understand the controlling factors of soil moisture response to rainfall in space. All included effects are listed in Table 1 (see above). We checked the normality of residuals with Q-Q plots and visually controlled the homogeneity of residuals at each fixed effect with box plots. Table 3 shows all fixed effects that govern soil-wetting patterns. The fixed effects contributed to the models more than the random effects. We calculated the full model R^2 as 0.88, while the contribution of the fixed effects to R^2 was 0.72 (Table 4). Weekly average wind speed, the spatial deviation of pre-event soil water content, and its interaction between seasonal and locational differences in grass height improved the model, yet they were not significant.

Gross precipitation had a significant positive relationship with the increase in soil water content at all locations, which means higher water input resulted in higher soil water content in the topsoil (Figure 3, Table 3). The spatial deviation of net precipitation from the mean (e.g., the spatial net precipitation pattern) had no effect on soil water content increase in the final model. Elevation of net precipitation measurement locations was significant with interaction with precipitation (Figure 3). The locations at higher elevations stored more water compared to lower places on the slope when relatively less weekly rainfall occurred, whereas this was reversed for more water input (Figure 4b).

TABLE 3 Summary of the linear mixed effects model for drivers of soil water content increase in the topsoil.

	t value	*p* value
Single fixed effects		
$\overline{P_g}$ (spatial mean of gross precipitation)	4.1	<0.001***
δh_{grass} (Spatial deviation of grass height)	−2.5	<0.05*
$\overline{\theta_{pre-ev,w}}$ (spatial mean of pre-event soil water content)	3.0	<0.01**
$\delta\theta_{pre-ev}$ (spatial deviation of pre-event soil water content)	1.8	0.077.
$\overline{u}$ (weekly mean wind speed)	1.5	0.19
Interaction fixed effects		
$\overline{P_g} \times Z_{\text{tube}}$	−3.5	<0.001***
$\overline{h_{\text{grass,w}}} \times \delta\theta_{\text{pre-ev,top-soil}}$	−1.6	0.11
$\delta h_{\text{grass}} \times \overline{\theta_{\text{pre-ev,w}}}$	4.5	<0.001***
$\delta h_{\text{grass}} \times \delta\theta_{\text{pre-ev}}$	1.5	0.13
Random effects (intercept)	−0.44	0.67

Note: All variables were measured and scaled with *Z* transformation before analysis. Satterthwaite's method was used for *t* tests. Significance codes are, '***' is ≈ 0, '**' is 0.001, '*' is 0.01, and '.' is 0.05.

TABLE 4 Overview of statistics for the linear mixed effects models shown in Figure 3

Topsoil	
AIC	162.27
R^2 full model	0.88
R^2 fixed	0.72
R^2 random	0.16

Note: Variables shown are: Adjusted R^2 and Akaike information criterion (AIC).

Average pre-event soil water content affected the increase in soil water content (Table 3, Figure 3). Soil water content increase was enhanced in times of wetter antecedent soil moisture status and suppressed during drier conditions (Figure 4c).

Spatial variation of the vegetation height directly affected the soil moisture response to rainfall. The spatial deviation of grass height from the mean (e.g., the spatial canopy height pattern) was a significant driver of the increase in soil water content. Specifically, at the locations with taller size grass, the increase in soil water content was relatively less (Figure 4d). However, the temporal change in average grass height was not a controlling factor for the increase in the local soil water content. Furthermore, the interaction between the spatial deviation of grass height and the antecedent soil moisture was significant, such that the dampening effect of grass height on soil water storage was mainly important in moderate and dry antecedent soil moisture conditions (Figure 4e). Overall, the dependence of the local grass height effect on the soil

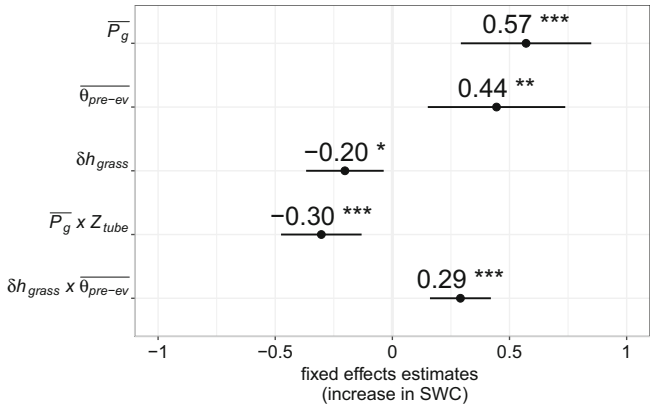

FIGURE 3 Fixed effect estimates of the weekly cumulative increase in soil water content (SWC) in the topsoil (0–17.5 cm) in the presence of the developed grass canopy (the result of the model shown in Table 3). Values on the *x*-axis indicate the slope of the relations. The shown predictors are weekly measured spatial mean gross precipitation ($\overline{P_g}$), weekly spatial average pre-event soil moisture status ($\overline{\theta_{\text{pre-ev}}}$), spatial deviation of pre-event soil moisture status ($\delta\theta_{\text{pre-event}}$), weekly spatial average grass height ($\overline{h_{\text{grass}}}$), spatial deviation of grass height (δh_{grass}), elevation of net precipitation measurement locations (Z_{tube}). Only significant effects are shown. All variables were scaled with *Z* transformation. Interaction is shown with '*x*'. Significance codes: '***' is ≈ 0, '**' is 0.001, '*' is 0.01, '.' is 0.05

moisture status indicates that the canopy also affects other processes besides interception loss.

4 | DISCUSSION

4.1 | No systematic effect of seasonal canopy growth on soil water content increase after rainfall

We demonstrated that gross precipitation was a significant driver of the increase in soil water content, as precipitation is the primary source of soil moistening, particularly for topsoil layers (Lozano-Parra et al., 2015; Salve et al., 2011; Zhang et al., 2020). In addition, we found that topography significantly influenced the soil moisture response depending on the size of weekly cumulated precipitation events. The latter may be caused by lateral flow, as topographically, lower elevations receive more water in larger rainfall events. Inclusion of this interaction term ($\overline{P_g} \times Z_{\text{tube}}$) in the model allowed us to control for the impact of lateral flow on soil wetting patterns and evaluate the remaining controlling factors independently of topography-driven dynamics.

Canopy development regulates how vegetation intercepts and redistributes rainfall as net precipitation components and interception loss are controlled by leaf, branch, and stem features (Pypker et al., 2011). Seasonal growth of grass typically relates to leaf and stem production and increased leaf area index (LAI) (Gusmão Filho et al., 2020; Macedo et al., 2021). Vegetation height is proportional to water storage in herbaceous vegetation canopies (Xiong et al., 2019). Thus, we expected that the seasonal change of canopy height in a grassland governs interception storage as well as the amount of water reaching the soil and, thereby, the increase in soil water storage (Crouse et al., 1966; Gilliam et al., 1987; Zou et al., 2015). Moreover, Demir et al. (2022) showed that local net precipitation in the same grassland site was governed by temporal and spatial variation of canopy height. However, in contrast to our expectations, neither spatial variation in net precipitation nor average grass height affected soil wetting patterns. We attributed this to two potential causes: (1) incomplete quantitative representation of net precipitation and/or (2) soil water dynamics obscuring the rainfall signal (see next section). Regarding (1), the water balance revealed that the collected net precipitation was lower than the water entering the soil, and this concerned all weeks with peak grass height, which indicates an under-catch of net precipitation. With the tubes being very reliable in terms of capturing dripping precipitation, the under-catch can most likely be attributed to missing stemflow (Demir et al., 2022).

Unfortunately, stemflow measurements in managed dense grasslands are not possible, but data from selected ecosystems and species show that stemflow in grass and crop species can be substantial (Lin et al., 2020). For instance, Seastedt (1985) measured average throughfall as 49% of gross precipitation for tallgrass prairie, and this portion increased to 75% with stemflow while others neglected the generated stemflow by the same grass type (Clark, 1940; Zou et al., 2015). Also, studies conducted in croplands confirm that, herbaceous vegetation can produce a substantial amount of stemflow (up to 23% of gross precipitation), which has been repetitively shown for varied crop types such as sorghum (e.g., Bui & Box, 1992), sugar cane (e.g., Fernandes et al., 2021), soybean (e.g., Timlin et al., 2001), maize (e.g., Bui & Box, 1992; Liu et al., 2015; Nazari et al., 2020; Paltineanu & Starr, 2000), rapeseed (Drastig et al., 2019) and potato cultivars (Deblonde et al., 1999; Jefferies & MacKerron, 1985; Saffigna et al., 1976).

Furthermore, from the little research that is available on grasslands, e.g., from the lab, it is known that stemflow production also in grasses is a function of length, width, number, and basal area of stems together with rainfall characteristics (De Ploey, 1982). Taller grasslands typically contain more elongated stems and flower tillers that allow gathering rain drops and propagating flow to the stem and into the ground rather than retaining it on the plant surfaces (Xiong et al., 2019). Hence the stemflow production probably increased as the grassland grew taller similar to croplands (Lin et al., 2020), which aligns with the mismatch of the water balance appearing at peak canopy development. We, therefore, conclude that the water balance mismatch is due to the under-catch of net precipitation potentially related to stemflow in this managed grassland; and hints that stemflow can alter the soil water balance even in grasslands. Therefore, quantifying stemflow in low-structured vegetation and understanding its role in below-ground water fluxes merits future investigations.

Additionally, soil water dynamics may have contributed to obscuring the signal of throughfall and interception loss, as discussed in more detail in the next section.

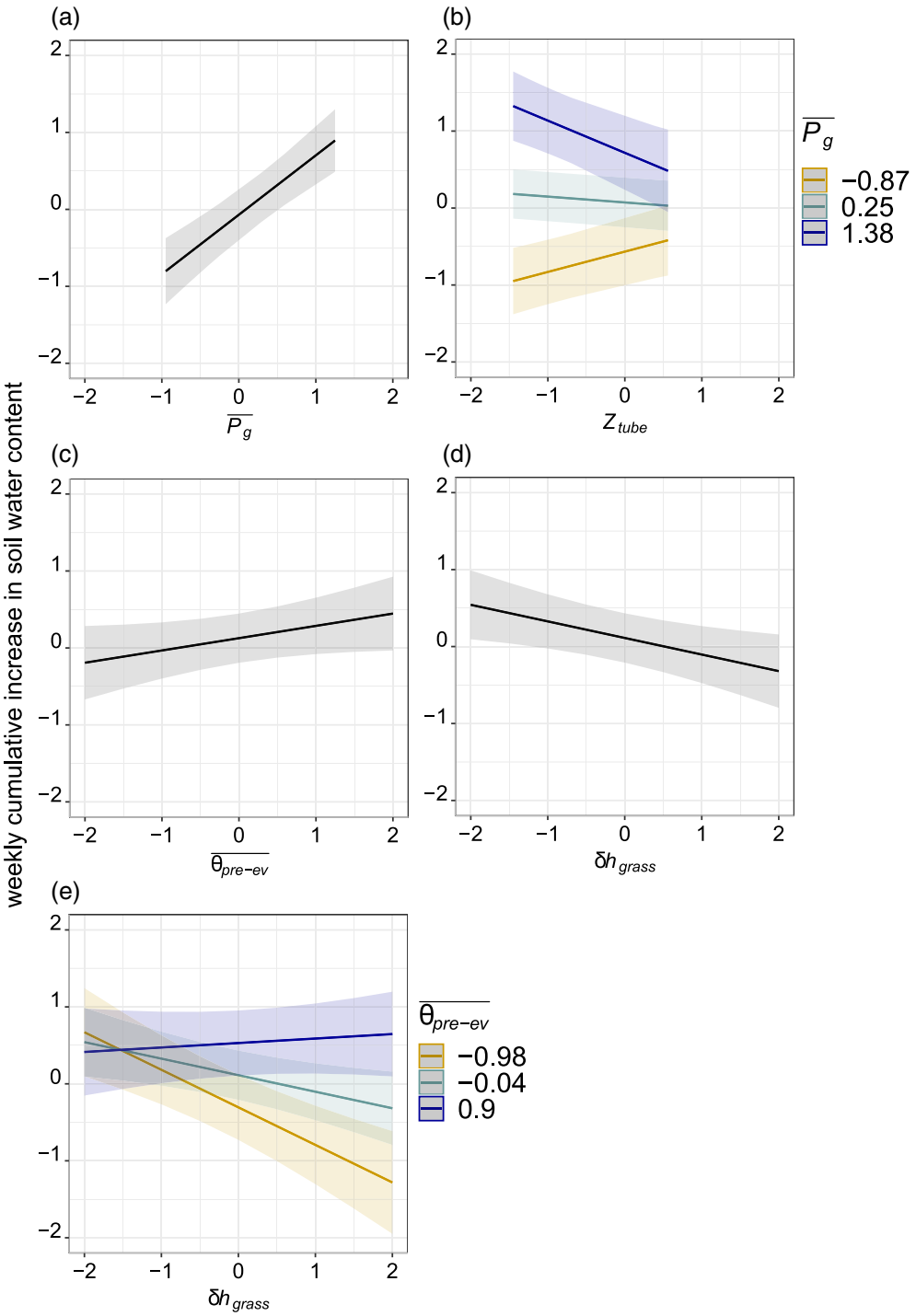

FIGURE 4 Significant relations of the linear mixed effects model estimation showed in Figure 3, representing the significant drivers of increase in soil water content (SWC) in the topsoil. Relation to (a) average gross precipitation ($\overline{P_g}$) and (b) the interactive relation of average gross precipitation ($\overline{P_g}$) and elevation of interception tubes (Z_{tube}). Relation to (c) average pre-event soil moisture status ($\overline{\theta_{pre-ev}}$), (d) spatial deviation of grass height (δh_{grass}). (e) Interactive relation of spatial deviation of grass height (δh_{grass}) and pre-event soil moisture status ($\overline{\theta_{pre-ev}}$)

4.2 | Antecedent soil moisture regulates soil water storage after rainfall

We found that temporal variation of antecedent soil water content governs soil moisture response to rainfall. Similarly, other studies showed that soil moisture changes are strongly affected by antecedent wetness status (Demand et al., 2019; Hardie et al., 2011; Merdun et al., 2008; Zehe et al., 2010; Zhu et al., 2014). Antecedent soil moisture conditions are known to regulate the infiltration process; thereby, the wetness status influences soil moisture response to rainfall (Zhang et al., 2020). Nevertheless, antecedent soil wetness status can affect soil moisture response in different ways. Zhu et al. (2014), for instance, found that the soil water content increased more notably under drier initial conditions compared to wetter conditions, especially after larger rain events. They attributed this observation to drier soil conditions freeing up the water holding capacity in the soil matrix. Likewise, other researchers argued that drier soil could store more water, whereas wetter soil conditions kick off preferential flow mechanisms (Beven & Germann, 1982; Jaynes et al., 2001; Kung et al., 2000). However, there is a growing consensus that dry soil

moisture status increases the occurrence of preferential flow even more than moist ones (Graham & Lin, 2011; Hardie et al., 2011; Nimmo, 2021; Ritsema & Dekker, 2000; Täumer et al., 2006; Yao et al., 2017), as we found with the statistical analysis.

The statistical model outcome revealed that soil moistening was enhanced in elevated pre-event soil water content, whereas drier pre-event conditions led to less storage and probably provoked rapid water drainage. Enhanced preferential flow paths by drier initial soil moisture status were also observed in other studies (Demand et al., 2019; Hardie et al., 2011; Merdun et al., 2008; Wiekenkamp et al., 2016). Dryness of antecedent soil moisture can result in water repellency (Doerr et al., 2000; Doerr & Thomas, 2003; Gimbel et al., 2016; Täumer et al., 2006) that reshapes preferential flow dynamics (Bauters et al., 2000; Jarvis et al., 2008). For instance, Demand et al. (2019) surmised that soil dryness resulted in the occurrence of preferential flow in their research site due to water repellency.

Grassland soils are prone to become water repellent because plant roots, fungi, and soil fauna release and distribute hydrophobic chemical compounds, particularly when soils dry out in summer, which amplifies preferential flow (Hallett et al., 2001; Lichner et al., 2011; Mao et al., 2016; Smettem et al., 2021). In fact, the soil under perennial grass can develop stronger water repellency than forest and other investigated crops (de Jonge et al., 2007). During our observation period, the topsoil volumetric water content decreased below 10% at the end of June and remained similarly low until the end of the observation period. Thus, the duration and level of dryness might have enhanced repellency and strengthened preferential flow paths later in the growing season.

Furthermore, we observed deep soil cracks, which became especially visible after the summer grass cut. Due to the summer cut, the soil surface was exposed to higher radiation and evaporation that widens and deepens soil cracks, as evaporation has an impact on soil cracking (Cordero et al., 2021). Drought and root water uptake can influence soil cracking, and the formed crack can remain through a series of wetting and drying cycles (Beven & Germann, 1982). Cracks are also known to enhance preferential flow or accelerate the rapid water flow (Beven & Germann, 1982; Hardie et al., 2011). Independently, the vegetation development and need for root growth as the soil dried might further have enhanced macropores (Beven & Germann, 1982). This additional macropore formation could intensify preferential flow paths along with the cracks. Overall, our results strongly indicate that preferential flow dominated soil water dynamics on the research site, particularly later in the season, and this may have masked the other signals in the soil moistening, such as interception and throughfall patterns.

4.3 | Spatial variation of grass height affects soil wetting patterns

Although seasonal evolution of grass height had no clear effect on the soil water response to rainfall, we found that spatial patterns of grass height had a significant effect. The mixed effects model revealed that locations with taller grass stored less soil water after rainfall. This is most likely attributed to interception loss. Interception loss is not uniform over space and time because of the spatio-temporal variation in canopy and rain event features (Crockford & Richardson, 2000; Gerrits et al., 2010). Canopy height is a controlling factor for interception loss in grasses (Breuer et al., 2003; Crouse et al., 1966). Relatively taller grass typically has a higher leaf area index, which can increase intercepted rainfall by the leaf surface and reduce throughfall formation. Our results manifested that variation in canopy height directly modulates soil wetting patterns by inducing spatial heterogeneity in water entering the soil. Secondly, below-ground growth progresses during the growing season and is probably more pronounced in locations where the grass is locally more productive (Li et al., 2008; Liu et al., 2021). Plant root systems are important for soil water dynamics as they shape soil particle orientation, form macropores due to root shrinkage or root decay, and also by root penetration and extension (Lu et al., 2020). In dye experiments, Li et al. (2009) observed that the occurrence of preferential flow is related to the presence of roots in shrubs in sandy soil. Higher biological activity and dense root networks in natural grasslands, similar to forests and shrubs, amplify the existence of macropores (Gonzalez-Sosa et al., 2010). Therefore, it is possible that non-uniform flow may be enhanced at locations with taller grass due to higher local macroporosity.

The statistical model result further indicated an interactive influence of spatial variation of grass height and antecedent soil wetness on soil moistening. The drier antecedent soil moisture the less water was stored in the soil in locations with taller grass, which suggests that the taller grass strengthened bypass flow under drier antecedent soil moisture conditions.

5 | CONCLUSIONS

In this study, we conducted field measurements to investigate the individual effect of antecedent soil moisture and canopy height along with throughfall patterns, gross precipitation, and weekly average wind speed in soil moisture response to rainfall. The results show that the spatial variation in canopy height governs soil wetting patterns, while the seasonal development of grass height does not. In addition, our results reveal a strong effect of the antecedent soil moisture conditions. Despite the potentially important role of average interception loss for the water balance, its effect on soil wetting patterns was probably weakened due to non-equilibrium flows. In our research site, average drier antecedent soil moisture conditions appear to cause preferential flow paths. Spatially varied canopy height introduced heterogeneity in water arriving at the soil surface and how it is stored.

Uneven vegetation development intensifies preferential pathways, particularly under drier and moderate pre-event soil wetness conditions. We surmise that the heterogeneous grassland canopy influenced the soil wetting patterns as it created spatial contrasts in water input. Notwithstanding the antecedent soil moisture conditions shaped how water was transported to the deeper subsurface, and

non-equilibrium flow probably dominated soil water dynamics obscuring the direct effect of throughfall patterns in soil moistening. Ultimately, these results confirm that spatial heterogeneity in canopy shapes soil moistening not only in forests but also even in grasslands.

ACKNOWLEDGEMENTS

This study is part of the Collaborative Research Centre (CRC 1076 AquaDiva) of the Friedrich Schiller University Jena, funded by the Deutsche Forschungsgemeinschaft (DFG, German Research Foundation)—SFB 1076—Project Number 218627073. We thank to AquaDiva subproject D03 for weather station (Reckenbuel) data. Also, people who contributed to installation of soil moisture sensors in the research site: Ricardo Ontiveros-Enriques, Bernd Ruppe, Danny Schelhorn, Josef Weckmüller. We thank the Hainich CZE site manager Robert Lehmann and the Hainich National Park. We thank the bachelor and master students Carla Peter, Xiaoyu Zhao, Stephan Bock. Open Access funding enabled and organized by Projekt DEAL.

DATA AVAILABILITY STATEMENT

The raw data supporting the conclusions of this article will be made available by the authors, without undue reservation.

ORCID

Gökben Demir https://orcid.org/0000-0002-1368-067X
Johanna Clara Metzger https://orcid.org/0000-0001-5630-9283

REFERENCES

Baroni, G. (2013). The role of vegetation and soil properties on the spatio-temporal variability of the surface soil moisture in a maize-cropped field. *Journal of Hydrology*, *489*, 148–159. https://doi.org/10.1016/j.jhydrol.2013.03.007

Bartoń, K. (2020). MuMIn: Multi-model inference. https://CRAN.R-project.org/package=MuMIn

Bates, D., Mächler, M., Bolker, B., & Walker, S. (2015). Fitting linear mixed-effects models using lme4. http://www.jstatsoft.org/v67/i01/

Bauters, T. W. J., Steenhuis, T. S., DiCarlo, D. A., Nieber, J. L., Dekker, L. W., Ritsema, C. J., Parlange, J.-Y., & Haverkamp, R. (2000). Physics of water repellent soils. *Journal of Hydrology*, *231–232*, 233–243. https://doi.org/10.1016/S0022-1694(00)00197-9

Beven, K., & Germann, P. (1982). Macropores and water flow in soils. *Water Resources Research*, *18*(5), 1311–1325. https://doi.org/10.1029/WR018i005p01311

Beven, K., & Germann, P. (2013). Macropores and water flow in soils revisited. *Water Resources Research*, *49*(6), 3071–3092. https://doi.org/10.1002/wrcr.20156

Bogena, H. R., Herbst, M., Huisman, J. A., Rosenbaum, U., Weuthen, A., & Vereecken, H. (2010). Potential of wireless sensor networks for measuring soil water content variability. *Vadose Zone Journal*, *9*(4), 1002–1013. https://doi.org/10.2136/vzj2009.0173

Bouten, W., Heimovaara, T. J., & Tiktak, A. (1992). Spatial patterns of throughfall and soil water dynamics in a Douglas fir stand. *Water Resources Research*, *28*(12), 3227–3233. https://doi.org/10.1029/92WR01764

Breuer, L., Eckhardt, K., & Frede, H.-G. (2003). Plant parameter values for models in temperate climates. *Ecological Modelling*, *169*(2–3), 237–293, 293. https://doi.org/10.1016/S0304-3800(03)00274-6

Bui, E. N., & Box, J. E. (1992). Stemflow, rain Throughfall, and erosion under canopies of corn and sorghum. *Soil Science Society of America Journal*, *56*(1), 242–247. https://doi.org/10.2136/sssaj1992.03615995005600010037x

Clark, O. R. (1940). Interception of rainfall by prairie grasses, weeds, and certain crop plants. *Ecological Monographs*, *10*(2), 243–277. https://doi.org/10.2307/1948607

Coenders-Gerrits, A. M. J., Hopp, L., Savenije, H. H. G., & Pfister, L. (2013). The effect of spatial throughfall patterns on soil moisture patterns at the hillslope scale. *Hydrology and Earth System Sciences*, *17*(5), 1749–1763. https://doi.org/10.5194/hess-17-1749-2013

Cordero, J. A., Prat, P. C., & Ledesma, A. (2021). Experimental analysis of desiccation cracks on a clayey silt from a large-scale test in natural conditions. *Engineering Geology*, *292*, 106256. https://doi.org/10.1016/j.enggeo.2021.106256

R Core Team. (2021). *R: The R project for statistical computing*. R Foundation for Statistical Computing https://www.r-project.org/

Crockford, R. H., & Richardson, D. P. (2000). Partitioning of rainfall into throughfall, stemflow and interception: Effect of forest type, ground cover and climate. *Hydrological Processes*, *14*(16–17), 2903–2920.

Crouse, R. P., Corbett, E. S., & Seegrist, D. W. (1966). Methods of measuring and analyzing rainfall interception by grass. *International Association of Scientific Hydrology Bulletin*, *11*(2), 110–120. https://doi.org/10.1080/02626666609493463

de Jonge, L. W., Moldrup, P., & Jacobsen, O. H. (2007). Soil-water content dependency of water Repellency In soils: Effect of crop type, soil management, and physical-chemical parameters. *Soil Science*, *172*(8), 577–588. https://doi.org/10.1097/SS.0b013e318065c090

De Ploey, J. (1982). A stemflow equation for grasses and similar vegetation. *Catena*, *9*(1), 139–152. https://doi.org/10.1016/S0341-8162(82)80010-6

Deblonde, P. M. K., Haverkort, A. J., & Ledent, J. F. (1999). Responses of early and late potato cultivars to moderate drought conditions: Agronomic parameters and carbon isotope discrimination. *European Journal of Agronomy*, *11*(2), 91–105. https://doi.org/10.1016/S1161-0301(99)00019-2

Demand, D., Blume, T., & Weiler, M. (2019). Spatio-temporal relevance and controls of preferential flow at the landscape scale. *Hydrology and Earth System Sciences*, *23*(11), 4869–4889. https://doi.org/10.5194/hess-23-4869-2019

Demir, G., Friesen, J., Filipzik, J., Michalzik, B., & Hildebrandt, A. (2022). A method proposal for throughfall measurement in grassland at plot scale in temperate climate: 'Interception tubes. *Frontiers in Earth Science*, *10*, 16. https://doi.org/10.3389/feart.2022.799419

Doerr, S. H., Shakesby, R. A., & Walsh, R. P. D. (2000). Soil water repellency: Its causes, characteristics and hydro-geomorphological significance. *Earth-Science Reviews*, *51*(1–4), 33–65. https://doi.org/10.1016/S0012-8252(00)00011-8

Doerr, S. H., & Thomas, A. D. (2003). Soil moisture: A controlling factor in water repellency? In C. J. Ritsema & L. W. Dekker (Eds.), *Soil water repellency* (pp. 137–149). Elsevier. https://doi.org/10.1016/B978-0-444-51269-7.50016-3

Drastig, K., Suárez Quiñones, T., Zare, M., Dammer, K.-H., & Prochnow, A. (2019). Rainfall interception by winter rapeseed in Brandenburg (Germany) under various nitrogen fertilization treatments. *Agricultural and Forest Meteorology*, *268*, 308–317. https://doi.org/10.1016/j.agrformet.2019.01.027

Dunkerley, D. (2000). Measuring interception loss and canopy storage in dryland vegetation: A brief review and evaluation of available research strategies. *Hydrological Processes*, *14*(4), 669–678.

Fernandes, R. P., da Costa Silva, R. W., de Andrade, T. M. B., Salemi, L. F., de Camargo, P. B., Martinelli, L. A., & de Moraes, J. M. (2021). Stemflow generation as influenced by sugarcane canopy development. *Environmental Monitoring and Assessment*, *193*(12), 789. https://doi.org/10.1007/s10661-021-09570-5

Gerrits, A. M. J., Pfister, L., & Savenije, H. H. G. (2010). Spatial and temporal variability of canopy and forest floor interception in a beech forest. *Hydrological Processes*, *24*(21), 3011–3025. https://doi.org/10.1002/hyp.7712

Gilliam, F. S., Seastedt, T. R., & Knapp, A. K. (1987). Canopy rainfall interception and throughfall in burned and unburned tallgrass prairie. *The Southwestern Naturalist*, *32*(2), 267. https://doi.org/10.2307/3671570

Gimbel, K. F., Puhlmann, H., & Weiler, M. (2016). Does drought alter hydrological functions in forest soils? *Hydrology and Earth System Sciences*, *20*(3), 1301–1317. https://doi.org/10.5194/hess-20-1301-2016

Gómez-Plaza, A., Alvarez-Rogel, J., Albaladejo, J., & Castillo, V. M. (2000). Spatial patterns and temporal stability of soil moisture across a range of scales in a semi-arid environment. *Hydrological Processes*, *14*(7), 1261–1277.

Gonzalez-Sosa, E., Braud, I., Dehotin, J., Lassabatère, L., Angulo-Jaramillo, R., Lagouy, M., Branger, F., Jacqueminet, C., Kermadi, S., & Michel, K. (2010). Impact of land use on the hydraulic properties of the topsoil in a small French catchment. *Hydrological Processes*, *24*(17), 2382–2399. https://doi.org/10.1002/hyp.7640

Graham, C. B., & Lin, H. S. (2011). Controls and frequency of preferential flow occurrence: A 175-event analysis. *Vadose Zone Journal*, *10*(3), 816–831. https://doi.org/10.2136/vzj2010.0119

Gusmão Filho, J. D., Deitos Fries, D., Maia de Lana Sousa, B., Lara Fagundes, J., Acosta Backes, A., Santos Dias, D. L., Campos Pinheiro, S. S., & Andrade Teixeira, F. (2020). Growth dynamics and senescence of digit grass as a response to several canopy heights. *Revista Mexicana de Ciencias Pecuarias*, *11*(1), 38–52. https://doi.org/10.22319/rmcp.v11i1.4913

Guswa, A. J. (2012). Canopy vs. roots: Production and destruction of variability in soil moisture and hydrologic fluxes. *Vadose Zone Journal*, *11*(3), vzj2011.0159. https://doi.org/10.2136/vzj2011.0159

Hallett, P. d., Baumgartl, T., & Young, I. m. (2001). Subcritical water repellency of aggregates from a range of soil management practices. *Soil Science Society of America Journal*, *65*(1), 184–190. https://doi.org/10.2136/sssaj2001.651184x

Hardie, M. A., Cotching, W. E., Doyle, R. B., Holz, G., Lisson, S., & Mattern, K. (2011). Effect of antecedent soil moisture on preferential flow in a texture-contrast soil. *Journal of Hydrology*, *398*(3), 191–201. https://doi.org/10.1016/j.jhydrol.2010.12.008

Jarecke, K. M., Bladon, K. D., & Wondzell, S. M. (2021). The influence of local and nonlocal factors on soil water content in a steep forested catchment. *Water Resources Research*, *57*(5), e2020WR028343. https://doi.org/10.1029/2020WR028343

Jarvis, N., Etana, A., & Stagnitti, F. (2008). Water repellency, near-saturated infiltration and preferential solute transport in a macroporous clay soil. *Geoderma*, *143*(3–4), 223–230. https://doi.org/10.1016/j.geoderma.2007.11.015

Jarvis, N. J. (2007). A review of non-equilibrium water flow and solute transport in soil macropores: Principles, controlling factors and consequences for water quality. *European Journal of Soil Science*, *58*(3), 523–546. https://doi.org/10.1111/j.1365-2389.2007.00915.x

Jaynes, D. B., Ahmed, S. I., Kung, K.-J. S., & Kanwar, R. S. (2001). Temporal dynamics of preferential flow to a subsurface drain. *Soil Science Society of America Journal*, *65*(5), 1368–1376. https://doi.org/10.2136/sssaj2001.6551368x

Jefferies, R. A., & MacKerron, D. K. L. (1985). Stemflow in potato crops. *The Journal of Agricultural Science*, *105*(1), 205–207. https://doi.org/10.1017/S0021859600055891

Jian, S., Zhang, X., Li, D., Wang, D., Wu, Z., & Hu, C. (2018). The effects of stemflow on redistributing precipitation and infiltration around shrubs. *Journal of Hydrology and Hydromechanics*, *66*(1), 79–86. https://doi.org/10.1515/johh-2017-0043

Klos, P. Z., Chain-Guadarrama, A., Link, T. E., Finegan, B., Vierling, L. A., & Chazdon, R. (2014). Throughfall heterogeneity in tropical forested landscapes as a focal mechanism for deep percolation. *Journal of Hydrology*, *519*, 2180–2188. https://doi.org/10.1016/j.jhydrol.2014.10.004

Kohlhepp, B., Lehmann, R., Seeber, P., Küsel, K., Trumbore, S. E., & Totsche, K. U. (2017). Aquifer configuration and geostructural links control the groundwater quality in thin-bedded carbonate–siliciclastic alternations of the Hainich CZE, Central Germany. *Hydrology and Earth System Sciences*, *21*(12), 6091–6116. https://doi.org/10.5194/hess-21-6091-2017

Kung, K.-J. S., Steenhuis, T. S., Kladivko, E. J., Gish, T. J., Bubenzer, G., & Helling, C. S. (2000). Impact of preferential flow on the transport of adsorbing and non-adsorbing tracers. *Soil Science Society of America Journal*, *64*(4), 1290–1296. https://doi.org/10.2136/sssaj2000.6441290x

Küsel, K., Totsche, K. U., Trumbore, S. E., Lehmann, R., Steinhäuser, C., & Herrmann, M. (2016). How deep can surface signals Be traced in the critical zone? Merging biodiversity with biogeochemistry research in a central German Muschelkalk landscape. *Frontiers in Earth Science*, *4*, 32. https://doi.org/10.3389/feart.2016.00032

Levia, D. F., & Frost, E. E. (2006). Variability of throughfall volume and solute inputs in wooded ecosystems. *Progress in Physical Geography: Earth and Environment*, *30*(5), 605–632. https://doi.org/10.1177/0309133306071145

Levia, D. F., & Germer, S. (2015). A review of stemflow generation dynamics and stemflow-environment interactions in forests and shrublands. *Reviews of Geophysics*, *53*(3), 673–714. https://doi.org/10.1002/2015RG000479

Li, X. Y., Yang, Z. P., Li, Y. T., & Lin, H. (2009). Connecting ecohydrology and hydropedology in desert shrubs: Stemflow as a source of preferential flow in soils. *Hydrology and Earth System Sciences*, *13*, 1133–1144.

Li, Y., Luo, T., & Lu, Q. (2008). Plant height as a simple predictor of the root to shoot ratio: Evidence from alpine grasslands on the Tibetan plateau. *Journal of Vegetation Science*, *19*(2), 245–252. https://doi.org/10.3170/2007-8-18365

Lichner, L., Eldridge, D. J., Schacht, K., Zhukova, N., Holko, L., Sir, M., & Pecho, J. (2011). Grass cover influences Hydrophysical parameters and heterogeneity of water flow in a Sandy soil. *Pedosphere*, *21*(6), 719–729. https://doi.org/10.1016/S1002-0160(11)60175-6

Lin, M., Sadeghi, S. M. M., & Van Stan, J. T. (2020). Partitioning of rainfall and sprinkler-irrigation by crop canopies: A global review and evaluation of available research. *Hydrology*, *7*(4), 76. https://doi.org/10.3390/hydrology7040076

Liu, H., Zhang, R., Zhang, L., Wang, X., Li, Y., & Huang, G. (2015). Stemflow of water on maize and its influencing factors. *Agricultural Water Management*, *158*, 35–41. https://doi.org/10.1016/j.agwat.2015.04.013

Liu, Y., Xu, M., Li, G., Wang, M., Li, Z., & De Boeck, H. J. (2021). Changes of aboveground and belowground biomass allocation in four dominant grassland species across a precipitation gradient. *Frontiers in Plant Science*, *12*, 609. https://doi.org/10.3389/fpls.2021.650802

Llorens, P., & Domingo, F. (2007). Rainfall partitioning by vegetation under Mediterranean conditions. A review of studies in Europe. *Journal of Hydrology*, *335*(1–2), 37–54. https://doi.org/10.1016/j.jhydrol.2006.10.032

Lozano-Parra, J., Schnabel, S., & Ceballos-Barbancho, A. (2015). The role of vegetation covers on soil wetting processes at rainfall event scale in scattered tree woodland of Mediterranean climate. *Journal of Hydrology*, *529*, 951–961. https://doi.org/10.1016/j.jhydrol.2015.09.018

Lu, J., Zhang, Q., Werner, A. D., Li, Y., Jiang, S., & Tan, Z. (2020). Root-induced changes of soil hydraulic properties: A review. *Journal of Hydrology*, *589*, 125203. https://doi.org/10.1016/j.jhydrol.2020.125203

Macedo, V. H. M., Cunha, A. M. Q., Cândido, E. P., Domingues, F. N., da Silva, W. L., Lara, M. A. S., & do Rêgo, A. C. (2021). Canopy structural variations affect the relationship between height and light interception in Guinea grass. *Field Crops Research*, *271*, 108249. https://doi.org/10.1016/j.fcr.2021.108249

Mao, J., Nierop, K. G. J., Rietkerk, M., Sinninghe Damsté, J. S., & Dekker, S. C. (2016). The influence of vegetation on soil water repellency-markers and soil hydrophobicity. *Science of the Total Environment*, *566–567*, 608–620. https://doi.org/10.1016/j.scitotenv.2016.05.077

Merdun, H., Meral, R., & Riza, D. A. (2008). Effect of the initial soil moisture content on the spatial distribution of the water retention. *Eurasian Soil Science*, *41*(10), 1098–1106. https://doi.org/10.1134/S1064229308100128

Metzger, J. C., Wutzler, T., Valle, N. D., Filipzik, J., Grauer, C., Lehmann, R., Roggenbuck, M., Schelhorn, D., Weckmüller, J., Küsel, K., et al. (2017). Vegetation impacts soil water content patterns by shaping canopy water fluxes and soil properties. Hydrological processes, *31*(22), 3783–3795. https://doi.org/10.1002/hyp.11274

Molina, A. J., Llorens, P., Garcia-Estringana, P., de las Heras, M. M., Cayuela, C., Gallart, F., & Latron, J. (2019). Contributions of throughfall, forest and soil characteristics to near-surface soil water-content variability at the plot scale in a mountainous Mediterranean area. *Science of the Total Environment*, *647*, 1421–1432. https://doi.org/10.1016/j.scitotenv.2018.08.020

Nazari, M., Sadeghi, S. M. M., Van Stan, J. T., & Chaichi, M. R. (2020). Rainfall interception and redistribution by maize farmland in Central Iran. *Journal of Hydrology: Regional Studies*, *27*, 100656. https://doi.org/10.1016/j.ejrh.2019.100656

Nimmo, J. R. (2021). The processes of preferential flow in the unsaturated zone. *Soil Science Society of America Journal*, *85*(1), 1–27. https://doi.org/10.1002/saj2.20143

Paltineanu, I. C., & Starr, J. L. (2000). Preferential water flow through corn canopy and soil water dynamics across rows. *Soil Science Society of America Journal*, *64*(1), 44–54. https://doi.org/10.2136/sssaj2000.64144x

Potthast, K., Meyer, S., Crecelius, A. C., Schubert, U. S., Tischer, A., & Michalzik, B. (2017). Land-use and fire drive temporal patterns of soil solution chemistry and nutrient fluxes. *Science of the Total Environment*, *605–606*, 514–526. https://doi.org/10.1016/j.scitotenv.2017.06.182

Pypker, T. G., Levia, D. F., Staelens, J., & Van Stan, J. T. (2011). Canopy structure in relation to hydrological and biogeochemical fluxes. In D. F. Levia, D. Carlyle-Moses, & T. Tanaka (Eds.), *Forest hydrology and biogeochemistry: Synthesis of past research and future directions* (pp. 371–388). Springer. https://doi.org/10.1007/978-94-007-1363-5_18

Ritsema, C. J., & Dekker, L. W. (2000). Preferential flow in water repellent sandy soils: Principles and modeling implications. *Journal of Hydrology*, *231–232*, 308–319. https://doi.org/10.1016/S0022-1694(00)00203-1

Sadeghi SMM, Gordon DA, Van Stan JT. 2020. A global synthesis of throughfall and stemflow hydrometeorology. In *Precipitation partitioning by vegetation: A global synthesis*, Van Stan I, John T, Gutmann E, Friesen J (Eds). Springer International Publishing: 49–70. DOI: https://doi.org/10.1007/978-3-030-29702-2_4

Saffigna, P. G., Tanner, C. B., & Keeney, D. R. (1976). Non-uniforminfiltration under potato canopies CI ausedby interception, Stemflow, and hilling. *Agronomy Journal*, *68*(2), 337–342.

Salve, R., Sudderth, E. A., St. Clair, S. B., & Torn, M. S. (2011). Effect of grassland vegetation type on the responses of hydrological processes to seasonal precipitation patterns. *Journal of Hydrology*, *410*(1–2), 51–61. https://doi.org/10.1016/j.jhydrol.2011.09.003

Seastedt, T. R. (1985). Canopy interception of nitrogen in bulk precipitation by annually burned and unburned tallgrass prairie. *Oecologia*, *66*(1), 88–92. https://doi.org/10.1007/BF00378557

Smettem, K. R. J., Rye, C., Henry, D. J., Sochacki, S. J., & Harper, R. J. (2021). Soil water repellency and the five spheres of influence: A review of mechanisms, measurement and ecological implications. *Science of the Total Environment*, *787*, 147429. https://doi.org/10.1016/j.scitotenv.2021.147429

Täumer, K., Stoffregen, H., & Wessolek, G. (2006). Seasonal dynamics of preferential flow in a water repellent soil. *Vadose Zone Journal*, *5*(1), 405–411. https://doi.org/10.2136/vzj2005.0031

Teuling, A. J., Hupet, F., Uijlenhoet, R., & Troch, P. A. (2007). Climate variability effects on spatial soil moisture dynamics. *Geophysical Research Letters*, *34*, L06406. https://doi.org/10.1029/2006GL029080

Teuling, A. J., & Troch, P. A. (2005). Improved understanding of soil moisture variability dynamics. *Geophysical Research Letters*, *32*, L05404. https://doi.org/10.1029/2004GL021935

Tian, J., Zhang, B., He, C., Han, Z., Bogena, H. R., & Huisman, J. A. (2019). Dynamic response patterns of profile soil moisture wetting events under different land covers in the mountainous area of the Heihe River watershed, Northwest China. *Agricultural and Forest Meteorology*, *271*, 225–239. https://doi.org/10.1016/j.agrformet.2019.03.006

Timlin, D., Pachepsky, Y., & Reddy, V. R. (2001). *Soil water dynamics in row and interrow positions in soybean (Glycine max L.)*. Springer.

Vachaud, G., Passerat De Silans, A., Balabanis, P., & Vauclin, M. (1985). Temporal stability of spatially measured soil water probability density function. *Soil Science Society of America Journal*, *49*(4), 822–828. https://doi.org/10.2136/sssaj1985.03615995004900040006x

Vereecken, H., Huisman, J. A., Pachepsky, Y., Montzka, C., van der Kruk, J., Bogena, H., Weihermüller, L., Herbst, M., Martinez, G., & Vanderborght, J. (2014). On the spatio-temporal dynamics of soil moisture at the field scale. *Journal of Hydrology*, *516*, 76–96. https://doi.org/10.1016/j.jhydrol.2013.11.061

Vereecken, H., Kamai, T., Harter, T., Kasteel, R., Hopmans, J., & Vanderborght, J. (2007). Explaining soil moisture variability as a function of mean soil moisture: A stochastic unsaturated flow perspective. *Geophysical Research Letters*, *34*(22), L22402. https://doi.org/10.1029/2007GL031813

Wiekenkamp, I., Huisman, J. A., Bogena, H. R., Lin, H. S., & Vereecken, H. (2016). Spatial and temporal occurrence of preferential flow in a forested headwater catchment. *Journal of Hydrology*, *534*, 139–149. https://doi.org/10.1016/j.jhydrol.2015.12.050

Xiong, P., Chen, Z., Yang, Q., Zhou, J., Zhang, H., Wang, Z., & Xu, B. (2019). Surface water storage characteristics of main herbaceous species in semiarid loess plateau of China. *Ecohydrology*, *12*(8), e2145. https://doi.org/10.1002/eco.2145

Yao, J., Cheng, J., Sun, L., Zhang, X., & Zhang, H. (2017). Effect of antecedent soil water on preferential flow in four soybean plots in southwestern China. *Soil Science*, *182*(3), 83–93. https://doi.org/10.1097/SS.0000000000000198

Zehe, E., Graeff, T., Morgner, M., Bauer, A., & Bronstert, A. (2010). Plot and field scale soil moisture dynamics and subsurface wetness control on runoff generation in a headwater in the Ore Mountains. *Hydrology and Earth System Sciences*, *14*(6), 873–889. https://doi.org/10.5194/hess-14-873-2010

Zhang, P., Xiao, P., Yao, W., Liu, G., & Sun, W. (2020). Profile distribution of soil moisture response to precipitation on the Pisha sandstone hillslopes of China. *Scientific Reports*, *10*(1), 9136. https://doi.org/10.1038/s41598-020-65829-w

Zhu, Q., Nie, X., Zhou, X., Liao, K., & Li, H. (2014). Soil moisture response to rainfall at different topographic positions along a mixed land-use hillslope. *Catena*, *119*, 61–70. https://doi.org/10.1016/j.catena.2014.03.010

Zimmermann, B., Zimmermann, A., Lark, R. M., & Elsenbeer, H. (2010). Sampling procedures for throughfall monitoring: A simulation study. *Water Resources Research*, *46*, W01503. https://doi.org/10.1029/2009WR007776

Zou, C. B., Caterina, G. L., Will, R. E., Stebler, E., & Turton, D. (2015). Canopy interception for a tallgrass prairie under Juniper encroachment. *Plos One*, *10*(11), e0141422. https://doi.org/10.1371/journal.pone.0141422

Zuur, A. F., Ieno, E. N., Walker, N., Saveliev, A. A., & Smith, G. M. (2009). *Mixed effects models and extensions in ecology with R*. Springer. https://doi.org/10.1007/978-0-387-87458-6

How to cite this article: Demir, G., Michalzik, B., Filipzik, J., Metzger, J. C., & Hildebrandt, A. (2022). Spatial variation of grassland canopy affects soil wetting patterns and preferential flow. *Hydrological Processes*, *36*(12), e14760. https://doi.org/10.1002/hyp.14760